

The physics of crêpes: Elasto-gravity control of soft folding

Tom Marzin^{1,2}, Barath Venkateswaran¹, Yuchen Xi¹, Sunghwan Jung² and P.-T. Brun³.

¹Department of Chemical and Biological Engineering, Princeton University, Princeton, NJ 08540, USA

² Department of Biological and Environmental Engineering, Cornell University, Ithaca, NY 14853, USA

³Department of Chemical Engineering, Soft Matter, Rheology and Technology (SMaRT), KU Leuven, Leuven, Belgium

(Dated: February 18, 2026)

Like a crêpe resting on a plate, a thin elastic sheet can fold smoothly under its own weight, forming reversible shapes without creases or imposed hinges. Such soft folds arise from a balance between elastic bending and gravity, yet their stability, packing limits, and dynamics remain poorly understood. Here we show that these behaviors are governed by a single physical length scale, the elasto-gravity length ℓ_{eg} . Using experiments and heavy-elastica theory, we demonstrate that ℓ_{eg} sets the characteristic fold geometry, determines when a fold becomes unstable and unfolds, and limits how many reversible folds can be stacked in rectangular and circular sheets. In particular, when lengths are rescaled by ℓ_{eg} , fold shapes and stability thresholds collapse across materials and thicknesses. We further show that unfolding follows a universal speed scaling $v \sim \sqrt{g \ell_{eg}}$, revealing a gravity-controlled time scale for the release of stored bending energy. Together, these results establish a unified physical framework for reversible folding, compact storage, and gravity-assisted deployment of thin elastic sheets.

Folding a sheet in half is a familiar operation, encountered in activities ranging from everyday handling to industrial packaging. In food preparation, for example, wraps such as tortillas or crêpes are routinely folded (Fig. 1a), while in manufacturing, thin sheets are folded or rolled to increase storage density and later enable deployment. In some contexts, folding is achieved by imposing sharp creases [1] or by applying external forces that fix the fold shape [2, 3]. By contrast, many thin sheets can also fold softly under their own weight, forming smooth and reversible configurations without creases (Fig. 1b). Whether such folds remain stable, or relax and reorganize, is governed not by yield or plasticity but by a subtle, nonlinear interplay among geometry, elastic bending, and gravity. Such folding behavior is particularly relevant in cases where large, thin sheets must be stored compactly without creases, thereby avoiding persistent damage from plasticity effects.

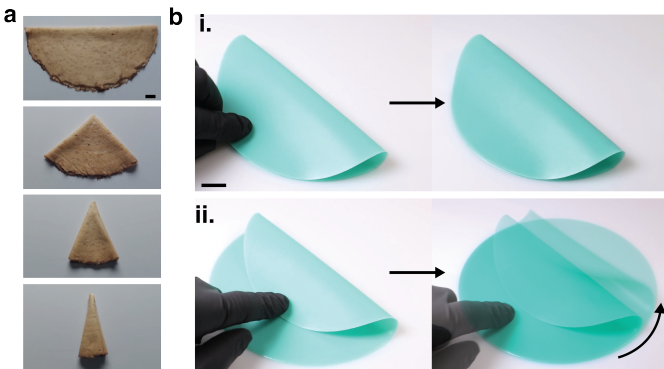


FIG. 1. Soft folding: a) Multi folded shape of a crêpe of radius $R \approx 13$ cm and $\ell_{eg} \approx 0.86$ cm. b) Elastomeric circular membrane of radius $R = 7.5$ cm and $\ell_{eg} = 1.99$ cm wrapped in two configurations: i) a symmetric half-fold that forms a stable loop, ii) an asymmetric, partial fold that is mechanically unstable and unravels upon release. (scale bars are 2 cm)

In many problems involving thin structures, the material's weight is assumed to be negligible. This is the case for inflated membranes, where tension and pressure dominate [4, 5], or for snapping instabilities in which elastic bending alone is key to elu-

cide the stability [6, 7]. Here, we instead consider heavy elastic sheets for which gravity directly competes with bending elasticity [8, 9]. Related competitions between bending and gravity have been explored in a variety of systems, including rucks in rugs [10, 11], gravity-induced buckling [12–14], and wrinkle or fold formation under confinement [15–18]. However, in contrast to origami-like creases [1, 19], compression-induced folds [7], or naturally curved slender systems [20, 21], where deformation is either localized or geometrically prescribed, folds in our system are not imposed. Instead, they emerge, migrate, and disappear through the interplay of bending, gravity, and frictional contact forces. As a first step towards understanding these temporary folds, we will predict whether a folded sheet will persist or spontaneously unfold.

In this Letter, we combine experiments and theory to characterize the static and dynamic behavior of soft folded states (Fig. 1b). In these configurations, part of the sheet rests flat on a rigid substrate, while the remaining portion lifts and bends out of plane before reconnecting with the flat region, forming a smooth and reversible fold. This soft folding mechanism is observed both in controlled polymer and plastic sheets and in familiar materials, including food samples such as crêpes and tortillas, for which multiple folds can be formed and stacked without creasing or permanent deformation (Fig. 1a). Here we show how the competition between bending stiffness and self-weight selects a characteristic fold size and determines whether a given folded state is stable or instead spontaneously unravels (Fig. 1b and Movie S1).

Beyond identifying stability criteria, we translate our results into practical design principles, e.g., for stacking multiple folds without triggering spontaneous release. We then demonstrate that, once stability is lost, unfolding occurs through a rapid conversion of bending and gravitational energy into motion, with characteristic speeds set by the elasto-gravity balance and the sheet's material properties. Together, these results provide a unified, mechanics-based framework for understanding soft folding in heavy elastic sheets. By connecting the behavior of familiar folded objects to underlying elastic principles, they offer both intuitive, pedagogical insight and practical design rules for gravity-mediated storage and deployment.

Fig. 2 reports on the stability of folded configurations with slen-

der elastic sheets (Shimstock Plastic Sheets, Artus) of thicknesses $h \in [25, 125]\mu\text{m}$, width $w = 6\text{ cm}$, lengths $L \in \{30, 50, 60\}\text{ cm}$, and Young's modulus $E = 4.76 \pm 0.46\text{ GPa}$. One end of each sheet is positioned onto a substrate. The other end is brought into contact with the flat portion of the sheet to create a soft *fold* (Fig. 2a-b), which is a smooth, reversible, arch-like configuration formed without creasing or plastic deformation. The primary control parameter is the end-to-end gap δ between the two contact points of the sheet, which is adjusted quasi-statically by gently sliding the upper layer (Fig. 2a-b). For each imposed value of δ , we measure the fold height H and the free length b , defined as the portion of the sheet not in contact with the substrate (Fig. 2c). An experiment terminates when the folded configuration loses stability and spontaneously unravels to the flat state. We denote this instability threshold by δ_- and record the corresponding values H_- and b_- . Note that when the gap is sufficiently large, $\delta > \delta_+$, the end portion of the sheet lies flat on the lower one, producing a finite dead length, similar to the elastocapillary racket [3]. These configurations are, by definition, stable.

We focus on the interval $\delta \in [\delta_-, \delta_+]$, for which a stable, well-defined fold without excess flat length exists. By balancing elastic and gravitational moment, we obtain an elasto-gravity length scale [8, 10, 22],

$$\ell_{eg} = \left(\frac{B}{\rho g w h} \right)^{1/3}, \quad (1)$$

where $B = Eh^3w/12(1 - \nu^2)$ is the sheet's bending stiffness, ρ the density of the sheet, and g the acceleration due to gravity. Considering an infinitesimal deformation ϵ and balancing the gravitational and bending moments, we have $\rho g h w \ell_{eg} \epsilon \sim B \epsilon / \ell_{eg}^2$, thereby recovering Eq. 1. Given the nature of our problem, we anticipate the relevance of ℓ_{eg} , which varies between 2.7 and 8.5, cm in our experiments (see SI). In Fig. 2c, we plot H/ℓ_{eg} and b/ℓ_{eg} versus δ/ℓ_{eg} . Our experimental data collapses across sheet thicknesses, indicating that fold shapes are indeed governed by ℓ_{eg} . In particular, $H \approx \ell_{eg}$ is a very good estimate for the fold height, regardless of the gap, a remarkably simple result.

In Fig. 2d, we report the dimensions of a fold near threshold. Remarkably, these values are nearly constant when rescaled by ℓ_{eg} . To further rationalize this observation, we model the free portion of the sheet as an inextensible *heavy* elastica. The sheet is uniform along its width w , and deformation is confined to the $x-y$ plane. The centerline is parameterized by a dimensionless arc-length $s \in [0, 1]$ rescaled by the *a priori*, unknown free length b . The coordinates are given by $x' = \cos \theta$ and $y' = \sin \theta$, where $\theta(s)$ is the angle made by the tangent to the centerline with the horizontal. Force resultants are written in dimensionless form as (n_x, n_y) , where n_x is the unknown horizontal force and $n'_y = (b/\ell_{eg})^3$ is the gravity component. Moment balance yields the second order heavy-elastica equation [8, 10, 23] (see SI for further details):

$$\theta'' + n_y \cos \theta - n_x \sin \theta = 0. \quad (2)$$

Closing the problem requires seven boundary conditions. In the absence of adhesion, the curvature vanishes at both contact lines, reflecting the absence of localized moments at these points [10, 11]. We thus have $x(0) = 0$, $y(0) = 0$, $\theta(0) = 0$ and $\theta'(0) = 0$, at the base $s = 0$; and $y(1) = 0$ and $\theta'(1) = 0$ at the free end

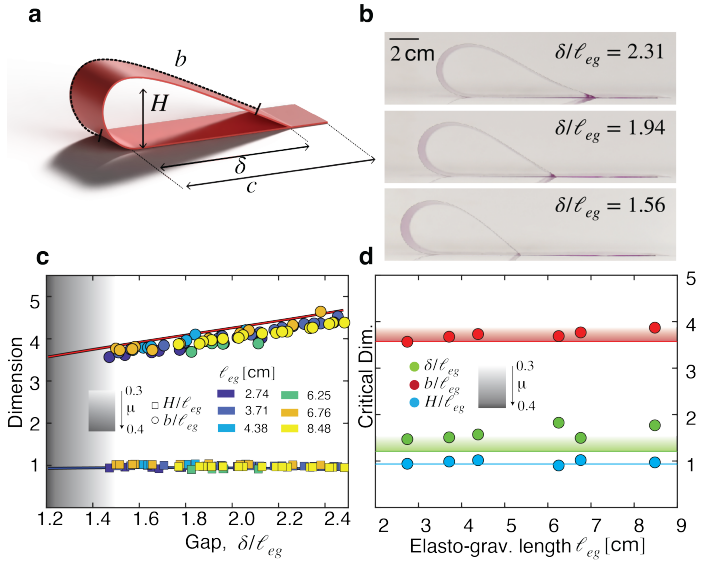


FIG. 2. Folding stability: a) Schematic of the soft folding geometry. b) Three representative folding configurations at different gap values δ , for a strip $L = 30\text{ cm}$ long and $t = 40\mu\text{m}$ thick ($\ell_{eg} = 3.71\text{ cm}$). c) Fold length and height as functions of the gap for various sheet thicknesses; all lengths are rescaled by the elasto-gravity length ℓ_{eg} . d) Dimensions of the fold at criticality (length, height, and gap) as functions of ℓ_{eg} . In c) and d), solid lines represent theoretical predictions, while shaded regions indicate the range expected from frictional effects.

$s = 1$. The end-to-end gap sets the final condition $x(1) = \delta$. As δ increases, loss of contact occurs when the vertical force at the upper contact vanishes, triggering unfolding. The model predicts this instability at $\delta_-/\ell_{eg} = 1.21$, with corresponding dimensions $b_-/\ell_{eg} = 3.57$ and $H_-/\ell_{eg} = 0.93$ (Fig. 2d).

In Fig. 2c-d, we show that the shapes obtained by integrating Eq. 2 are mostly in favorable agreement with experiments. However, we observe a small yet systematic deviation in our estimates of b and δ . In effect, experiments suggest that the transition occurs at $\delta_-^{exp}/\ell_{eg} \approx 1.61 \pm 0.15$, which corresponds to $b_-^{exp}/\ell_{eg} \approx 3.71 \pm 0.1$ (see Fig. 2d). This discrepancy suggests the presence of an additional instability mechanism. Thus, we impose another stability criterion, based on frictional forces acting on the free end. Using Coulomb friction, a surface with static friction coefficient μ can support horizontal forces at the sheet's free end without slipping, up to a certain threshold, i.e., $|n_x| < \mu |n_y|$. Including this constraint in our model, we find that low static friction coefficients lead to a premature loss of stability, as the upper layer slips over the lower layer before lifting off. The corresponding friction-limited region is shown by the shaded bands in Fig. 2d for $0.3 \lesssim \mu \lesssim 0.4$. Experiments indicate a transition around $\mu \approx 0.28 \pm 0.04$, consistent with reported friction values for similar materials [24, 25]. Notice that for sufficiently large friction ($\mu > 0.39$), the model predicts that the sheet can only undergo a flip instability rather than slipping.

We now turn to large values of δ , beyond which both extremities of the loop lie flat on the substrate. This critical gap is obtained by integrating Eq. 2. We find $\delta_+/\ell_{eg} = 2.48$, while experiments yield a slightly larger value, $\delta_+^{exp}/\ell_{eg} = 2.63 \pm 0.16$. The corresponding free lengths are $b_+/\ell_{eg} = 4.68$ in theory and

$b_+^{exp}/\ell_{eg} = 4.69 \pm 0.29$ experimentally (see SI for experimental points), showing good agreement in this regime.

Beyond stability, the geometry of a soft fold determines its capacity to enclose material. We quantify this capacity through the volume enclosed by the folded configuration. Measurements and predictions from Eq. 2 show good agreement across all sheet thicknesses (see graph and derivation details in SI). Notably, the enclosed volume varies non-monotonically with the imposed gap δ and reaches a maximum at an optimal shift $\delta_* = 2.02 \ell_{eg}$. At this optimum, the volume reaches $1.51 \ell_{eg}^2 w$, irrespective of the material thickness. Experiments yield $\delta_*^{exp} = (2.18 \pm 0.15) \ell_{eg}$ and a corresponding volume $(1.62 \pm 0.13) \ell_{eg}^2 w$, confirming the existence of an optimal fold that maximizes enclosed capacity while remaining mechanically stable. Next, we examine the stability of stacked soft folds.

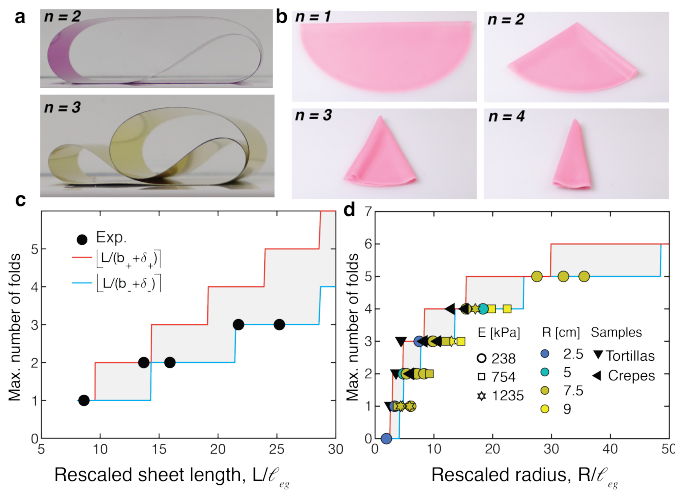


FIG. 3. Stacking folds: a) Snapshots of multi-folding states for rectangular sheets with $\ell_{eg} = 3.71$ cm and $\ell_{eg} = 2.4$ cm, respectively. b) Snapshots of multi-folding states for a circular soft sheet (for $R = 7.5$ cm and $\ell_{eg} = 4.8$ cm), where the sector angle α is halved at each fold. c) Maximum number of times a rectangular strip (width $w = 6$ cm and length $L = 60$ cm) can be folded as a function of the rescaled length L/ℓ_{eg} . d) Maximum fold count for circular sheets (crêpes) against rescaled radius R/ℓ_{eg} . In a) and c), contour lines show the geometric prediction; the gray band indicates the admissible range for the fold to be stable.

In Fig. 3, we report results related to the stability of multi-stack folded configurations for both rectangular and circular sheets made from PET plastic, VPS elastomer, and food samples. For the rectangular case, a ribbon of dimensions $(L \times w) = (60 \text{ cm} \times 6 \text{ cm})$ is folded in half end-to-end, then folded again, and so on, until the configuration becomes unstable and unwraps spontaneously. In Fig. 3a we show the maximum fold count sustained by the sheet as a function of the rescaled length L/ℓ_{eg} . A smaller ratio yields fewer folds, ranging from 1 fold for the thickest sheets ($h = 125 \mu\text{m}$) to 3 folds for the thinnest ($h = 25 \mu\text{m}$).

An estimate of the maximum number of folds follows from our previous single-fold analysis and the integration of Eq. 2. We argue that each fold spans a length ranging from $\delta_- + b_- = 4.8 \ell_{eg}$ and $\delta_+ + b_+ = 7.2 \ell_{eg}$. As such, the number of folds is bounded by the nearest integers obtained by dividing the sheet length by these limits. In Fig. 3c, we show that this approach captures all experimental data points, although here the number of folds re-

mains modest. In order to increase the number of folds, we move to circular sheets, as detailed next.

We work with circular sheets with radius R (see SI for fabrication details). The folding procedure halves the sector angle α at each step, as illustrated in Fig. 3b. After n folds, the sector angle is $\alpha \approx \pi/2^{n-1}$. In experiments, we vary both the crêpe's radius $R \in [2.5, 9]$ cm and its elasto-gravity length ℓ_{eg} , which by Eq. (1), depends on the thickness $h \in [0.06, 0.97]$ mm and the Young's modulus $E \in \{228, 884, 1101\}$ kPa of the sheet. In Fig. 3c, we report the maximum fold number sustained by the sheet. We find that larger radii and smaller values of ℓ_{eg} allow for a greater number of folds. In addition to synthetic elastomer sheets, we report data points obtained from industrial food samples, including crêpes and tortillas, as shown in Fig. 1a. Despite their inherent material heterogeneity, these comestible sheets fall within the same stability envelope as the elastomer samples when rescaled by their elasto-gravity lengths (see Fig. 3c), evidencing the robustness of this process.

To rationalize these observations, we use a geometric argument. Each fold halves the sector angle, so that after n folds the available sector area scales as $S \sim \alpha R^2$. Stability requires that the area swept by the folded loop, estimated from the characteristic fold size set by ℓ_{eg} , remains smaller than the available sector area. This criterion yields a closed-form estimate for the maximum fold count $n(R/\ell_{eg})$, which is reported as the stability envelope in Fig. 3c (see SI for derivative details).

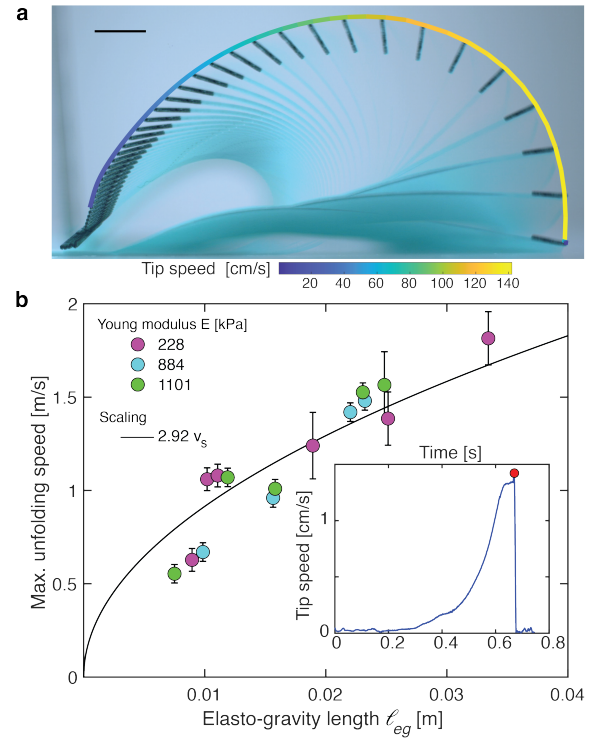


FIG. 4. Dynamics of unfolding: a) Chronophotography of the unfolding dynamics for $\ell_{eg} = 2.2$ cm ($E = 884$ kPa, $h = 1.13$ mm), the solid line reports the tip trajectory and the color modulates the instantaneous speed. Scale bars are 1 cm. b) Peak flipping speed as a function of elasto-gravity length [inset: full kinematics of the sample shown in b), red point is the maximal speed].

We note that the folding protocol used for circular sheets introduces a localized geometric singularity at the tip of the folded sector, after the second fold. This singularity appears to be confined to a small region near the apex and affects the overall dynamics across the parameter range explored in this study.

Overall, experiments across all sheet types are well captured by these simple geometric and mechanical arguments. Most data fall closer to the lower bound of the predicted stability range, reflecting the requirement that a stable fold retain a finite flat segment, which increases the material length consumed by each fold. This geometric reasoning parallels Gallivan's approach for estimating the maximum number of localized creases in paper sheets [26–28].

Finally, we investigate the unwrapping dynamics of a folded elastomer sheet (length $L \in [10, 12]$ cm, $\delta \approx \delta_- \approx 1.21 \ell_{eg}$) and record its motion with a high-speed camera (Chronos 1.4, Kron Technologies - 1069 and 1397 fps). In Fig. 4a, we show a representative chronophotography where the trajectory of the tip is highlighted. We observe a progressive increase in the tip speed, leading to a peak value $v_* \approx 1.47$ m/s attained shortly before the tip impacts the floor (see inset of Fig. 4b). In Fig. 4b, we report the evolution of v_* with ℓ_{eg} ($0.2 \leq h \leq 1.22$ mm), and observe its increase from 0.5 m/s to nearly 2 m/s.

We rationalize this dynamics by considering the sum of the bending energy when folded, $E_b \sim Bb\ell_{eg}^{-2}$ and of the gravitational potential energy $E_g \sim \rho ghwb^2$, and equate this sum to the kinetic energy in the course of deployment $E_k \sim \rho hwbv_s^2$. Using Eq. (1) and $b \sim \ell_{eg}$ from Fig. 2d, we obtain $v_s \simeq 2.14\sqrt{g\ell_{eg}}$, a scaling that also dictates the traveling speed of a ruck in a rug [10]. (see SI for derivation details). In Fig. 4b, this scaling is verified with data across all thicknesses and elastomer types, confirming the role of the elasto-gravity in setting a universal time scale for free unfolding. Note that the prefactor differs, as we find $v_s^{exp} \simeq 2.92\sqrt{g\ell_{eg}}$, a discrepancy that is expected given the crude approximation made in our derivation.

To conclude, we note that a single parameter governs the mechanics of soft folding in heavy elastic sheets: the elasto-gravity length ℓ_{eg} . Overall, this Letter provides a unified framework for understanding and designing soft folds, from single-loop stability to multi-fold packing and elastically powered actuation.

ACKNOWLEDGEMENTS

All the authors acknowledge Lauren Dreier, Andrej Košmrlj, Yicong Fu, Crystle Fowler, and Hongsik Kim for helpful discussions; Dominique Marzin for performing the crêpe experiments in Brittany; and Marjorie Batard-Kerviel for the crêpe recipe and cooking advice.

[1] Théo Jules, Frédéric Lechenault, and Mokhtar Adda-Bedia. Local mechanical description of an elastic fold. *Soft matter*, 15(7):1619–1626, 2019.

[2] Joseph D Paulsen, Vincent Démery, Christian D Santangelo, Thomas P Russell, Benny Davidovitch, and Narayanan Menon. Optimal wrapping of liquid droplets with ultrathin sheets. *Nature materials*, 14(12):1206–1209, 2015.

[3] Charlotte Py, Paul Reverdy, Lionel Doppler, José Bico, Benoit Roman, and Charles N Baroud. Capillary origami: spontaneous wrapping of a droplet with an elastic sheet. *Physical review letters*, 98(15):156103, 2007.

[4] DR Merritt and F Weinhaus. The pressure curve for a rubber balloon. *American Journal of Physics*, 46(10):976–977, 1978.

[5] Dominic Vella, Amin Ajdari, Ashkan Vaziri, and Arezki Boudaoud. Wrinkling of pressurized elastic shells. *Physical review letters*, 107(17):174301, 2011.

[6] Michael Gomez, Derek E Moulton, and Dominic Vella. Critical slowing down in purely elastic ‘snap-through’ instabilities. *Nature Physics*, 13(2):142–145, 2017.

[7] Tom Marzin, Barath Venkateswaran, Thomas Baroux, and P-T Brun. Augmented snap-through instability of folded strips. *Physical Review Research*, 7(1):013330, 2025.

[8] C.Y. Wang. A critical review of the heavy elastica. *International Journal of Mechanical Sciences*, 28(8):549–559, January 1986. Publisher: Elsevier BV.

[9] Adriano A Batista. The mechanics of bending a strip of paper. *European Journal of Physics*, 41(6):065009, 2020.

[10] Dominic Vella, Arezki Boudaoud, and Mokhtar Adda-Bedia. Statistics and Inertial Dynamics of a Ruck in a Rug. *Physical Review Letters*, 103(17), October 2009. Publisher: American Physical Society (APS).

[11] John M Kolinski, Pascale Aussillous, and Lakshminarayanan Mahadevan. Shape and motion of a ruck in a rug. *Physical review letters*, 103(17):174302, 2009.

[12] Matteo Taffetani, Finn Box, Arthur Neveu, and Dominic Vella. Limitations of curvature-induced rigidity: How a curved strip buckles under gravity. *Europhysics Letters*, 127(1):14001, 2019.

[13] Djebar Baroudi, Ivan Giorgio, Antonio Battista, Emilio Turco, and Leonid A. Igumnov. Nonlinear dynamics of uniformly loaded *Elastica*: Experimental and numerical evidence of motion around curled stable equilibrium configurations. *ZAMM - Journal of Applied Mathematics and Mechanics / Zeitschrift für Angewandte Mathematik und Mechanik*, 99(7):e201800121, July 2019.

[14] Marie Tani, Joo-Won Hong, Takako Tomizawa, Étienne Lepoivre, José Bico, and Benoît Roman. Curvy cuts: Programming axisymmetric kirigami shapes. *Extreme Mechanics Letters*, 71:102195, 2024.

[15] Fabian Brau, Pascal Damman, Haim Diamant, and Thomas A. Witten. Wrinkle to fold transition: influence of the substrate response. *Soft Matter*, 9(34):8177, 2013. Publisher: Royal Society of Chemistry (RSC).

[16] Stéphanie Deboeuf, Suzie Protière, and Eytan Katzav. Yin-yang spiraling transition of a confined buckled elastic sheet. *Physical Review Research*, 6(1):013100, 2024.

[17] Silas Alben. Packing of elastic rings with friction. *Proceedings of the Royal Society A*, 478(2258):20210742, 2022.

[18] Benny Davidovitch and Vincent Démery. Rucks and folds: delamination from a flat rigid substrate under uniaxial compression. *The European Physical Journal E*, 44(2):11, 2021.

[19] Frederic Lechenault, Benjamin Thiria, and Mokhtar Adda-Bedia. Mechanical response of a creased sheet. *Physical review letters*, 112(24):244301, 2014.

[20] A. C. Callan-Jones, P.-T. Brun, and B. Audoly. Self-Similar Curling of a Naturally Curved Elastica. *Physical Review Letters*, 108(17):174302, April 2012.

[21] Octavio Albarrán Arriagada, Gladys Massiera, and Manouk Abkarian. Curling and rolling dynamics of naturally curved ribbons. *Soft Matter*, 10(17):3055–3065, 2014.

- [22] Douglas P Holmes. Elasticity and stability of shape-shifting structures. *Current opinion in colloid & interface science*, 40:118–137, 2019.
- [23] Teodor M Atanackovic. *Stability theory of elastic rods*, volume 1. World Scientific, 1997.
- [24] Keisuke Yoshida and Hirofumi Wada. Mechanics of a snap fit. *Physical Review Letters*, 125(19):194301, 2020.
- [25] Tomohiko G Sano, Emile Hohnadel, Toshiyuki Kawata, Thibaut M  t  vet, and Florence Bertails-Descoubes. Randomly stacked open cylindrical shells as functional mechanical energy absorber. *Communications Materials*, 4(1):59, 2023.
- [26] Britney C Gallivan. *How to Fold Paper in Half Twelve Times: An Impossible Challenge Solved and Explained*. Historical Society of Pomona Valley, 2002.
- [27] Erik D Demaine, David Eppstein, Adam Hesterberg, Hiro Ito, Anna Lubiw, Ryuhei Uehara, and Yushi Uno. Folding a paper strip to minimize thickness. In *International Workshop on Algorithms and Computation*, pages 113–124. Springer, 2015.
- [28] Gaurish Korpal. Say crease! folding paper in half miles please. *At Right Angles*, 4(3):20–23, 2015.